IEEE Access
Multidisciplinary ⋮ Rapid Review ⋮ Open Access Journal

Received 17 March 2023, accepted 4 April 2023, date of publication 12 April 2023, date of current version 19 April 2023.

Digital Object Identifier 10.1109/ACCESS.2023.3266511

RESEARCH ARTICLE

Lightweight EfficientNetB3 Model Based on Depthwise Separable Convolutions for Enhancing Classification of Leukemia White Blood Cell Images

AMREEN BATOOL[1] **AND YUNG-CHEOL BYUN**[2]
[1]Department of Electronic Engineering, Institute of Information Science and Technology, Jeju National University, Jeju 63243, South Korea
[2]Department of Computer Engineering, Institute of Information Science and Technology, Jeju National University, Jeju 63243, South Korea

Corresponding author: Yung-Cheol Byun (ycb@jejunu.ac.kr)

This work was supported by the Ministry of Small and Medium-Sized Enterprises (SMEs) and Startups (MSS), South Korea, under the Regional Specialized Industry Development Plus Program (Research and Development) supervised by the Korea Technology and Information Promotion Agency for SMEs (TIPA) under Grant S3246057.

ABSTRACT Acute lymphoblastic leukemia (ALL) is a type of leukemia cancer that arises due to the excessive growth of immature white blood cells (WBCs) in the bone marrow. The ALL rate for children and adults is nearly 80% and 40%, respectively. It affects the production of immature cells, leading to an abnormality of neurological cells and potential fatality. Therefore, a timely and accurate cancer diagnosis is important for effective treatment to improve survival rates. Since the image of acute lymphoblastic leukemia cells (cancer cells) under the microscope is complicated to recognize the difference between ALL cancer cells and normal cells. In order to reduce the severity of this disease, it is necessary to classify immature cells at an early stage. In recent years, different classification models have been introduced based on machine learning (ML) and deep learning (DL) algorithms, but they need to be improved to avoid issues related to poor generalization and slow convergence. This work enhances the diagnosis of ALL with a computer-aided system that yields accurate results by using DL techniques. This research study proposes a lightweight DL-assisted robust model based on EfficientNet-B3 using depthwise separable convolutions for classifying acute lymphoblastic leukemia and normal cells in the white blood cell images dataset. The proposed lightweight EfficientNet-B3 uses less trainable parameters to enhance the performance and efficiency of the leukemia classification. Furthermore, two publicly available datasets are considered to evaluate the effectiveness and generalization of the proposed lightweight EfficientNet-B3. In addition, different measures are employed, such as accuracy, precision, recall, and f1-score, to evaluate the effectiveness of the proposed and baseline classifiers. In addition, a detailed analysis is given to evaluate and compare the performance and efficiency of the proposed with existing pre-trained and ensemble DL classifiers. Experimental results show that the proposed model for image classification achieves better performance and outperforms the existing benchmark DL and other ensemble classifiers. Moreover, our finding suggests that the proposed lightweight EfficientNet-B3 model is reliable and generalized to facilitate clinical research and practitioners for leukemia detection.

INDEX TERMS Acute lymphoblastic leukemia (ALL), efficientnet-B3, CNN, white blood cell image classification, deep learning.

The associate editor coordinating the review of this manuscript and approving it for publication was Vicente Alarcon-Aquino.

I. INTRODUCTION

Leukemia is a type of blood cancer that affect the white blood cells to become cancerous. The immune system of the body is facing the risk of these abnormal blood cells, which affect the bone marrow and white and red blood cells. Bone marrow cancer affects children and teenagers. Acute leukemia has two types: ALL and acute myeloid leukemia (AML). Lymphocytes, a type of immature white blood cell into the normal cells, multiply uncontrollably in the bone marrow in ALL; they are further divided into three subtypes, L1, L2, and L3; cells are typically tiny and have similar shapes. Acute lymphoblastic leukemia is the most common type of leukemia in children.

Blood cells can become contaminated with cancerous cells, which can infiltrate multiple organs and cause harm to the body [1]. If the rapid growth of abnormal cells isn't detected and treated in time, bone marrow depletion can lead to severe complications. The risk gradually decreases until the late 20s, when it begins to rise again. According to the American Cancer Society, ACS estimates 6660 cases of ALL in the US in 2022 children and adults. The ALL risk is high in children younger than five years old [2]. However, the majority of ALL occurs in adults. Chemotherapy, radiation, and anti-cancer drugs are treatments for leukemia depending on the patient's symptoms and risk level. They are primarily concerned with treating patients or alleviating symptoms of the disease. The life expectancy of ALL patients has been extended by developing several therapeutic strategies. Patients' age, health status, and severity determine the best treatment [3]. In addition to stem cell transplantation, patients in remission may also be able to receive this treatment. The standard treatment for ALL is chemotherapy, which prevents damage to the central nervous system. When analyzing ALL molecular features and cell morphology used [4].

Several morphological characteristics distinguish healthy cells from ALL cells, including cell size, nucleus size, nucleus colour distribution, nucleus texture, cytoplasm size, number of nucleoli in the nucleus, nucleus contour, boundary, and cytoplasm condition [5]. This disease can present with minor symptoms such as fever, gum bleeding, exhaustion, dizziness, and bone pain, up to severe life-threatening symptoms, depending on the bone marrow involvement [6], [7]. There was about a 1:5 and a 2:5 nucleus-to-cytoplasm ratio in healthy cells. Smear cells with a regular nuclear shape and size are homogeneous and uniform, round to oblong, and tiny in size [8]. Without proper treatment, ALL is a deadly disease; if not treated well, it spreads quickly in children's bodies. Therefore, leukemia diagnosis requires classifying the white blood cells in the bone marrow. The classification of white blood cell images presented several challenges. ALL blast cells and normal cells are difficult to identify because of their similarities. The CNN technique is one of the most advanced and popular computer vision techniques to efficiently utilize for different tasks related to processing image data [9], [10]. Various medical imaging applications successfully used pre-trained neural networks like ResNet, VGGnet, and Inception. CNN also used transfer learning in which huge generic datasets were trained and then trained on specific classification on a smaller dataset, a problem prevalent in medical datasets.

Many researchers proposed various techniques and algorithms for the detection of leukemia classifications. Although there are still some limitations in this area, the challenges of the current work motivate this study.

The following are the key contributions of the suggested lightweight model:

- A robust lightweight EfficientNet-B3 model is developed based on depthwise separable convolutions for accurate and reliable classification of leukemia cells.
- Two datasets are considered as a case study to present a detailed effectiveness analysis for ensuring the reliability and generalization of the proposed lightweight EfficientNet-B3 model.
- The detailed empirical analysis is presented to evaluate the effectiveness and efficiency of the proposed lightweight EfficientNet-B3 model for accurate binary and multi-class classification of leukemia cells.
- In addition, a comprehensive analysis is presented to evaluate and compare the performance and efficiency of the proposed lightweight EfficientNet-B3 and existing state-of-the-art DL classifiers.

Furthermore, the remaining research article of our proposed architecture is organized in such sections, such as section II discusses the related work, and section III describes the proposed framework of methods and materials. The data description, preprocessing, and analysis are provided in section III-A. Section IV describes the experimental setup and results analysis and compares the proposed approach with other current techniques, while V concludes the article.

II. RELATED WORK

Several studies have been performed on white blood cells to classify them. Traditional image processing techniques and machine learning models are used for the classification. This section presents existing leukemia detection classification methods using in-depth features and feature extraction methods. Blood cell classification has been the subject of extensive research, especially in developing modern CNNs. On the large majority of datasets, accuracy has gradually increased over time. The impact of early detection in cancer treatment clarifies this work's significance. There are many automated computer-based systems for pattern detection, but their speed and accuracy are not good [11], [12], [13]. Feature extraction algorithms such as speed-up Robust Feature [14], [15], [16], Scale Invariant Feature Transform [17], histogram of oriented gradients [18], and grey level co-occurrence matrices [19] is used for feature selection, and extraction, but there are some limitations in this methods. CNN was used for this process and achieved high accuracy.

TABLE 1. Summary of literature review.

Model	Year	Highlights	Challenges
WBC Leukemia Detection Method [20]	2022	Lighting and its variations in the behavioral analysis do not affect the technique.	The Proposed method is robust, but it is not efficient as DL.
GAN+ResNet [21]	2022	The ResNet and GAN algorithms achieved the highest accuracy and solved the problem of missing images.	Different labeling procedures and development stages can cause cell aberrations and misdiagnosis.
V-GAN & AC-GAN [22]	2021	V-GAN provides images that resemble true blood cell images & AC-GAN improve classifier performance environment.	AC-GAN faces a problem producing image augment with the training set classifier development. If a significant proportion of the enhanced photographs are duplicates, the classifier will be trained on a less diverse dataset.
Pretraind VGG16 with DCED [23]	2022	The proposed method uses whole-slide image segmentation rather than single-cell segmentation.	Several applications, including scene categorization, require a considerable amount of labeled data. Millions of annotated images are needed to solve these difficulties, but they are not readily available.
DLabV3+ResNet50 [24]	2021	The technique reported here produces optimally segmented cell edges, resulting in more exact identification.	The database does not contain any records of leukocyte agglomerates. Moreover, the quality of the actual data used determines the precision of the training. Research in the future will focus on improving methods for a dataset containing images with leukocyte agglomerates.
ResNet50 with UNet [25]	2021	ESNET-50 was trained with a pre-adapted loss function that assisted in solving the vanishing gradient problem and improving segmentation quality.	Cell instance segmentation has a limitation in terms of distinguishing nearby cells and identifying distinct cells.

Furthermore, preprocessing stage involves pixel labelling, colour space conversion, and pixel fusion in WBCs [26]. Detecting acute leukemia using a K-mean clustering technique and converting RGB images into LAB and CMYK models in image format has been developed to resolve the image acquisition, detection, and segmentation issue [27]. After preprocessing pictures to find ROI, optimize them with histogram equalization and Wiener filtering [19]. According to [28], HoG descriptors and LR extract features for leukemia prediction using the ALL-IDB dataset. The author of [29] examined colour and texture data extracted from 2852 histograms using threshold and watershed approaches. An analysis of the relative impact of different feature extraction techniques [30]. SURF describes how to mine features from query-coloured images. Combining the SURF technique with GA [31] increased performance metrics and resulted in 92% feature extraction accuracy. There are three detectors: SIFT [32], FAST [33], and CenSurE [34]. A feature fusion strategy can also improve performance measurements by integrating hand-crafted features [35].

In addition, It is possible to recognize objects using traditional segmentation methods, quantitative and qualitative feature extraction and feature matching [36]. Due to low resilience, there are some limitations. By utilizing convolutional neural networks, efficient classification can be prepared using automatic feature extraction [37], [38], [39], [40], [41]. In deep learning methods [42], [43], [44], [45], pre-trained models such as AlexNet, GoogleNet [46], ResNet [47], VGG-16 [48], Inception V3 [49], and many others extract and select features. Based on the simulation of electron spectra for surface analysis (SESSA) algorithm, Ahmed et al. Proposed a method for extracting WBCs features using a robust CNN architecture called VGGNet. Jagadev and Virani present a strategy for categorizing leukemia cell images [50] and an SVM classification method is used in [50] for the detection of leukemia cells. The author of [51] proposed another approach to identify ALL using SVM classifiers. In [52], the author uses K-means clustering and support vector machines to recognize ALL cells in microscopic images [53], [54], [55].

Recent literature has applied deep learning-based techniques to categorize ALLs with significant results. CNNs and custom CNNs have been successfully used to train and test some cell categorization tasks [56]. In [57] a weighted ensemble approach of CNN is used to detect ALL in microscopic images. However, some of the main limitations of these approaches are needed to be improved, such as low efficiency, learning procedure, accurate detection rate, etc. Furthermore,

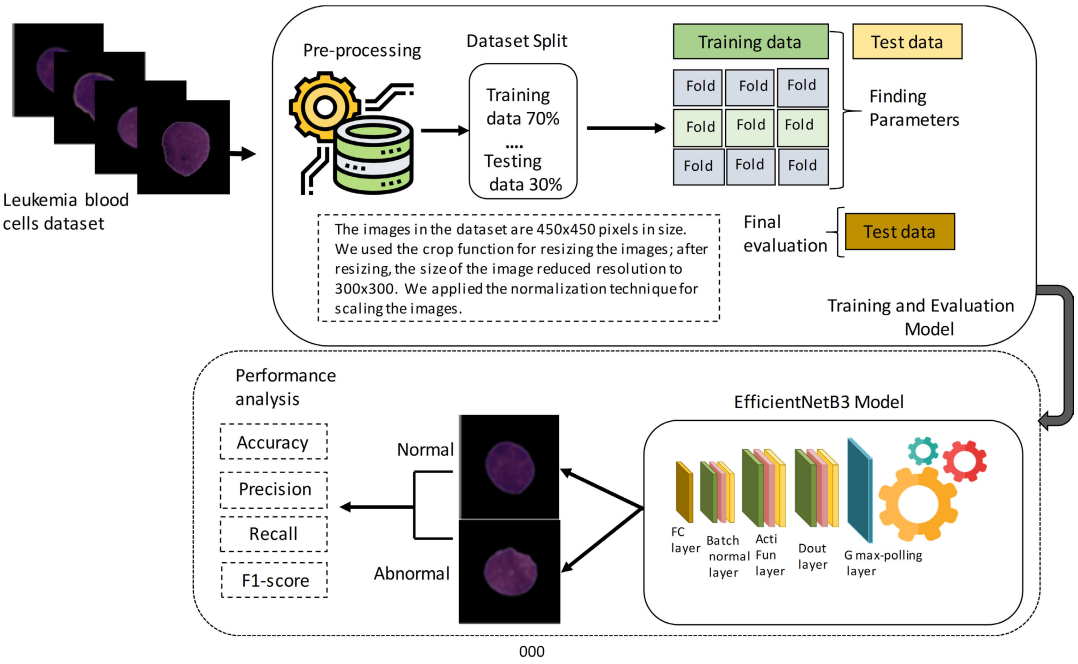

FIGURE 1. Description of proposed methodology.

these scratch CNN-based DL architectures require a large number of image samples, which are inadequate to acquire from a real-world domain. Therefore, in this way, transfer learning (TL) accomplished a significant potential to utilize pre-trained DL architectures for ALL classifications. However, pre-trained models, such as AlexNet, VGG-16, ResNet, etc., have several limitations, including complex architectures having several new hyper-parameters, low efficiency in terms of computational overhead, and feature discriminability among both normal and ALL images. Therefore, a new lightweight DL approach based on TL is needed to cope with these challenges and develop a reliable solution for leukemia cancer classification.

Therefore, We used deep learning techniques to classify recent developments in diagnosing lymphoblastic leukemia. We proposed A robust, lightweight model, which is used to recognize benign and malignant Leukemia cells accurately and reliably automatically, and classification techniques to assist researchers in understanding the latest advancements in leukaemia diagnosis. Additionally, many complex challenges and future research scopes are discussed.

III. METHOD AND MATRIALS

This section explains the detailed methodology of the proposed research study. Fig. 1 describes the proposed method in detail. In this study, we first collect the data set from the open-source publicly available dataset. After collecting the dataset, we preprocess the data and annotation. After the preprocessing, we need to create the proposed model EfficientNet-B3 for Leukemia classification. Our classification model used the pre-trained EfficientNet-B3 and trained it with a fully connected layer (FCL). Finally, we have evaluated our model with evaluation metrics.

A. DATA ACQUISITION AND DESCRIPTION

In this study, we used publicly available datasets such as C_NMC_2019 and acute lymphoblastic leukemia (All) datasets. The C_NMC_2019 dataset consists of 15,114 images of ALL collected from 118 subjects. Each picture has a 450 × 450 pixels resolution with a black background. Similarly, All dataset consists of all subtypes of malignant leukemia, such as benign, early, pre, and pro. All dataset images are captured using a Zeiss camera and also provide segmented images using a colour thresholding-based segmentation approach. In this way, binary and multi-class classification is employed to detect leukemia to highlight the significance of the deep learning (DL) based robust classifiers.

There are three parts to the dataset: training, primary test, and final test. Our evaluation tests utilized only the train and primary test sets because truth labels were present only in those two sets. Figure 2 describes the detailed dataset description; Fig. 3 shows images of normal blood cells and ALL blood cells.

These images were split into training and testing. The image dataset contains both normal and ALL blast cells. As part of this work, we used the labelled data from 45 subjects, namely, 4039 normal lymphocytes and 9817 blast lymphocytes. These images were split into training validation and test sets.

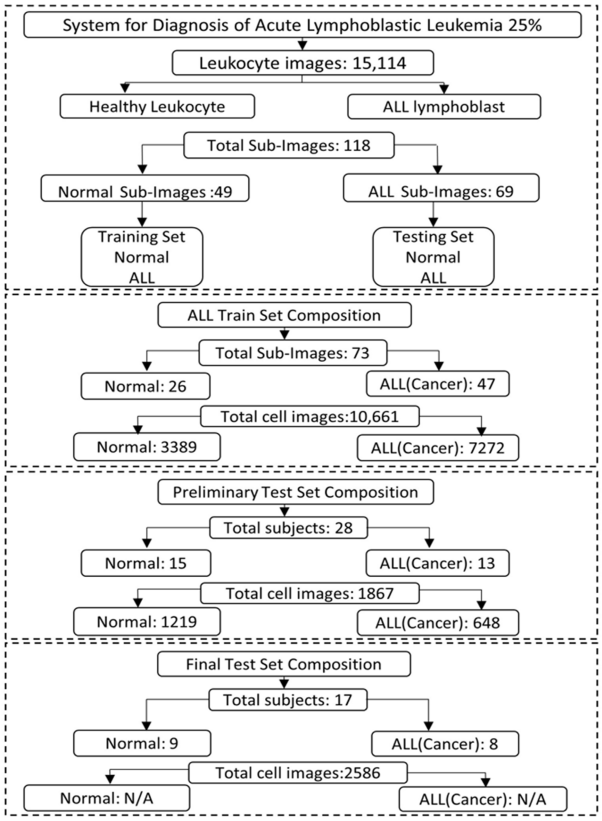

FIGURE 2. Description of the dataset and its splitting into training and testing sets.

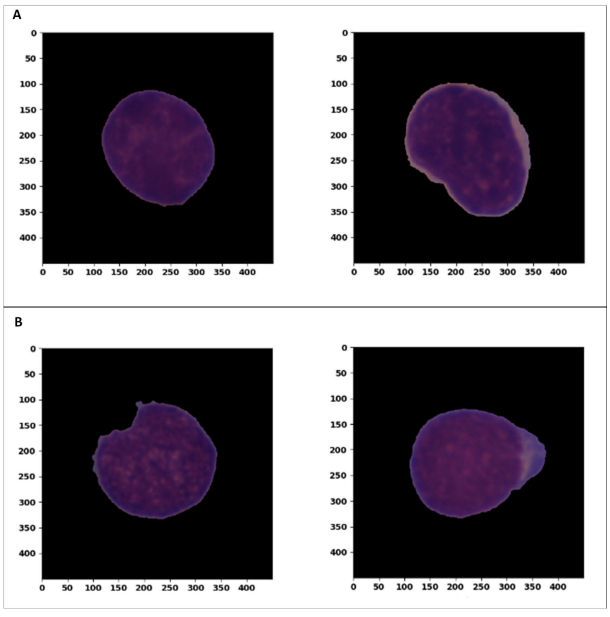

FIGURE 3. ALL leukemia blast cells and normal blood cells.

B. DATASET PREPROCEESING

The images in the dataset are 450 × 450 pixels in size. We used the TensorFlow crop function, the tf. image.crop_and_resize() for resizing the images; after this, the size of the image reduced resolution to 300 × 300. We applied the Min-Max normalization approach This normalization method scales the pixel values to be between 0 and 1. Mathematically, it is defined as:

Pixel normalized = (pixel - min_pixel_value) / (max_pixel_value - min_pixel_value)

where min_pixel_value and max_pixel_value are the minimum and maximum pixel values in the image.

C. DATA AUGMENTATION

Data augmentation is a technique used to generate additional training data by applying various transformations to the existing images in a dataset. We used ImageDataGenrator; this can be useful for increasing the size of the dataset and reducing overfitting in the classification model. In the context of the classification of white blood cell leukemia using deep learning-based features, some common data augmentation techniques include:

- **Rotation:** Images can be rotated by a random angle to simulate different directions we rotate image data in a range of 20.
- **Flipping:** Images can be horizontally or vertically flipped to simulate different viewpoints.
- **Zooming:** Images can be zoomed in or out by a random factor to simulate different scales. The zooming range of the image is 0.2.
- **Width _shift _range** The image shifted in the range of 0.2 left or right by up to half of its total width. It can be useful for increasing the diversity of training data and help to better generalize the model. Width shift range augments the image in both directions.
- **Height _shift _range** This parameter is used to randomly shift the height of an image. The image shifted upward or downward in the range of .2 by up to half of the actual size of the image.

D. EfficientNet

Efficient-Net was first introduces in [58]. The EfficientNet uses a cutting-edge CNN model scaling technique. Simple compound coefficients are used to achieve effective results. As opposed to conventional methods, which increase a network's breadth, depth, and resolution, EfficientNet consistently scales each dimension. The performance of models is improved when each size is scaled, but the performance is significantly enhanced when each network characteristic is balanced about resource availability. As a result of the equations, the authors [58] systematically increased the resolution of the image, and also the coefficient of depth, and width.

$$\text{Depth:} d = \alpha\varphi \tag{1}$$

$$\text{Width} : w = \beta\varphi \tag{2}$$

$$\text{Resolution} : r = \gamma\varphi \tag{3}$$

$$\text{s.t. } \alpha \cdot \beta 2 \cdot \gamma 2 \approx 2 \quad \alpha \geq 1, \beta \geq 1, \gamma \geq 1 \tag{4}$$

The coefficient φ regulates the access of novel resources for scaling the model. An initial grid α, β, and γ search

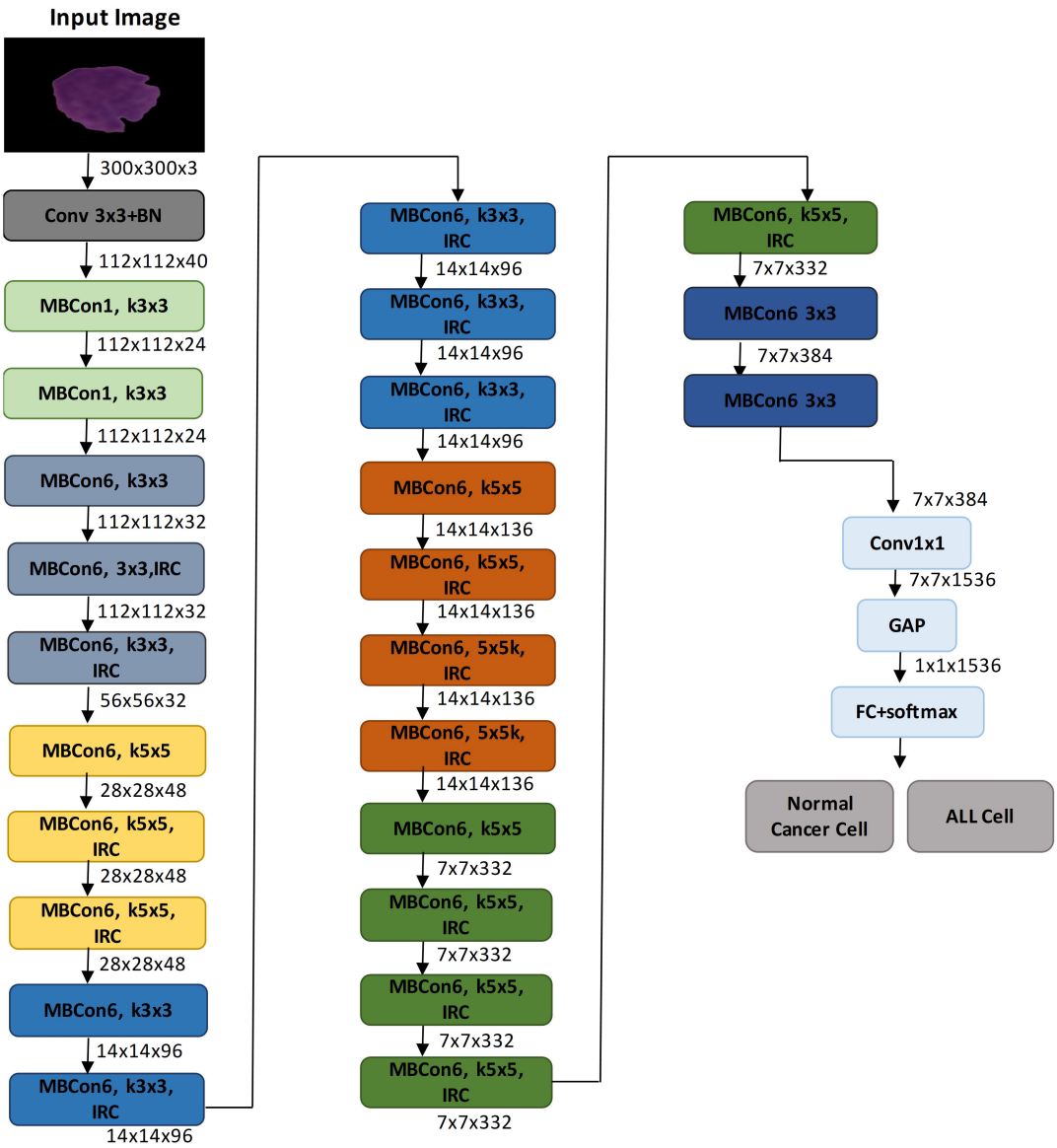

FIGURE 4. The effecientNet-B3 architecture illustrated 10,3646 million weights. The term IRC stands for inverted residual connection.

can identify these constants that define how the additional resources are allocated to the depth, width, and resolution.

E. PROPOSED ARCHITECTURE EfficientNet-B3

We propose to use the EfficientNetB3 version to balance the excellent performance and the running time. EfficientNet is a family of convolutional neural network architectures developed by Google Research. EfficientNet-B3 is one of the models in the EfficientNet family, which is considered a balanced and efficient model. One of the critical innovations of EfficientNet-B3 is using a compound scaling method to automatically scale up the model's architecture, in terms of depth (number of layers) and width (number of filters per layer), based on the input image resolution. This model allows us to use more resources when processing large and small images and perform better results and efficiency. The EfficientNet-B3 is the third model in the EfficientNet family, and it has the same depth as the EfficientNet-B0 but with 1.3 times the width and 1.2 times the resolution. The model can capture more fine-grained details in the input images due to having more filters per layer and a higher spatial resolution. Thus, the model has more filters per layer and a higher spatial resolution of the feature maps. The model consists of stacked convolutional layers interspersed with batch normalization layers and ReLU activation functions. Feature maps are also convolutional using depthwise separable convolutions, reducing the number of parameters by performing one convolution per channel. Using this approach, the model can

capture more complex patterns in input data while maintaining a relatively small parameter set. With the EfficientNet-B3, less computation is used to achieve better accuracy instead of the exact calculation for worse accuracy. Compared to the B1, the B3 uses depthwise separable convolutions, which make the model more efficient and result in a smaller model size, quicker inference, and lower memory usage. Over 1000 classes of objects are classified using the EfficientNet-B3 training dataset, ImageNet. This way, a great deal of data has been gathered to train the model, which can be fine-tuned or used for other tasks such as object detection, semantic segmentation, and transfer learning. Using three parameters to scale depth, width, and resolution, EfficientNet-B3 is a cost-efficient, robust model. In this architecture, 26 convolution blocks are followed by a convolution layer with batch normalization activation. An MB-Convolution is an inverted residual block (a convolution layer, then a depth-wise convolution, and then a convolution layer with skip connections at the beginning and end). After that, the dimensions' latent spaces are minimized through a global average pooling.

In this research work, we propose an efficient technique based on the EfficientNet-B3. We chose this specific Efficient Net variation because it offers a fair balance of accuracy and computing resources. Several other effective variations can use the same principles. Using the model scaling concept, other EfficientNet models are deeper and wider. As an example, Figure 4 shows the EfficientNet-B3 model, where IRC represents the inverted residual connection used by the MBConv block. It uses the same MBConv1 and MBConv6 modules as EffeicienNetB0. The inverted residual link is not used in all (IRC) modules. The abbreviation IRC stands for the modules that use this connection type. The other modules cannot connect because their input and output sizes are different, and it is impossible to perform an additional function

The input layer depicted the first CNN layer. Consider the image's input size of 300 × 300 pixels and its dimension of 3. EfficientNet-B3's architecture is comprised of several CNN layers. The training phase layer is flattened, dropout, and predicted dense layer. The dropout rate for our dropout layer is 0.3. The model has 11386829 parameters in all. Only the 11220445 can be trained, and the other remaining parameters, 87303, are not trained.

- EfficientNet-B3 (Functional) is a convolutional neural network with pre-trained weights, with an output shape of (None, 10, 10, 1536) and 10783535 parameters
- Global average pooling 2D 5 is a pooling layer that takes the average of each feature map across the spatial dimensions of the input and resulting (None, 1536).
- Flatten5 flatten the output from the previous layer to a one-dimensional tensor of shape (None, 1536).
- Dropout5 is used for reducing overfitting by randomly dropping neurons during training with a rate of 0.5.
- Dense4 is a fully connected layer with five units; it is a final output layer with 7685 parameters.

For extending the architecture of EfficientNet-B3 by adding Global Average Plloing2D Flatten and drop rate .45 to reduce over-fitting and Soft-max layer with two classes 0 and 1. The architecture optimized for 3050 sample images in 20 epochs, the learning rate is .001, and the Adamx optimizer is used for faster network optimization.

TABLE 2. Modified EfficientNet-B3 architecture for classification of leukemia blood cells images.

Layer (type)	Output shape	Parameter
EfficientNet-B3 (Functional)	(None) (10,10,1536)	10783535
Global average pooling 2D 5(Pooling)	(None, 1536)	0
Flatten-5 (Flatten)	(None, 1536)	0
Dropout-5 (Dropout)	(None, 1536)	0
Dense-4 (Dense)	(None, 5)	7685

TABLE 3. The summary of the settings of our training hyper-parameters.

Hyper_Parameters	Values
Loss_Function	MSE
Optimizer	Adamax
Batch_Size	40
Epoch	20

The given model uses the Mean Squared Error as its loss function. MSE is a commonly used loss function for regression problems, where the goal is to minimize the difference between the predicted output and the true output. The optimizer used for this model is Adam. Adam is an adaptive learning rate optimization algorithm that uses the gradient of the loss function to update the parameters of the model. It computes adaptive learning rates for each parameter. In general, Adam can be a good choice when the data is noisy. The batch size is 40, which means that 40 training examples will be used to compute the gradients before updating the model's parameters. This is an important hyper-parameter that can affect the speed and performance of the model. Larger batch sizes can lead to faster training but also more memory consumption. The number of epochs is 20, which means that the model will be trained on the entire dataset for 20 iterations. The training will be stopped after 20 iterations or epochs. It's worth noting that, depending on the complexity of the problem and the performance of the model, you may need to experiment with different values for these hyper-parameters in order to achieve the best performance.

IV. EXPERIMENTAL ENVIRONMENT, AND RESULTS ANALYSIS

This section provides extensive information regarding the dataset, experiments, model training, and model validation. The section also includes a performance comparison between the suggested technique and earlier work.

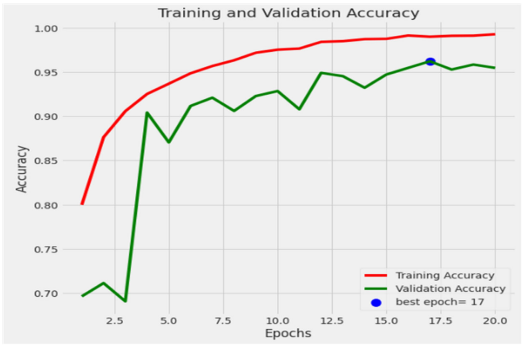

FIGURE 5. Training and validation accuracy.

FIGURE 6. Training and validation loss.

A. EXPERIMENTAL SETUP

The image size varies over datasets 300 × 300 image size is generally common. In this study, we resize the datasets to reduce training time and consistency. The dataset is randomly split into two phases, the training phase, and the testing phase. We tested the splits of 30%-70%, where the first 30% is the testing percentage, and the additional 70% of data is used for training.

- The learning rate of a hyper-parameter indicates how often the weights of the network will change after back-propagation.
- Our learning rate is set at 0.001 if the monitor value does not improve, the learning rate is reduced by a factor.
- We set 20 epochs for the training of the data, and the batch size is 40.
- For the first 5 epochs, the learning rate parameter is set to 0.001, and for the following 15 epochs, it is dropped to 0.0001.
- In the validation set, the model is saved with height accuracy.
- Adamax optimizer is used for training purposes with the extension of Adam that combines the best parts of the optimizer. In some conditions, the Adamax optimizer provides better results than the Adam optimizer.
- All the experiments were conducted in the Google Colab with machine learning library TensorFlow [59] written in Python.

B. PERFORMANCE OF PROPOSED MODEL

After the model was developed, we measured the performance of EfficientNte-B3 the data set was divided into training and validation. There are 9594 training photos in all and 526 for validation. The initial learning rate is 0.001, and the batch size was 40. The training finally started with 20 epochs.

Fig. 5 shows the model training and validation accuracy. Our model's training accuracy started at the first epoch slightly above 76% and validation accuracy at just below 72%. Training and validation accuracy increases to 92% and 88%, respectively, after just five epochs. After epoch 15, our model starts to stabilize a little bit. The accuracy changes for numerous epochs before ending with 99.31% after 20 epochs and 97.7% accuracy for validation.

Similarly, Fig. 6 shows that the loss graph for training and validation is almost the opposite of training and validation accuracy for example when accuracy increased then the loss decreased. In this condition, training and validation losses start at 65% and 58%, respectively. It rapidly decreased during the 20 epoch and declined below after the 20 epoch.

Furthermore, various algorithms have been used in the classification of ALL and normal leukaemia. There are many performance measures [60] that have been calculated to conduct a valid assessment between the models and the feature selection technique to validate the effectiveness of the proposed classifier. The performance measures as accuracy, precision, recall, F1-score, and specificity [61], necessary metrics for binary classification evaluation.

The following parameters are calculated in the evaluation metric.

1) **True Positive** (*TP*) Identifies abnormal cell leukemia samples that are correctly classified.
$\frac{TP}{Actualtrueclass}$
2) **True Negatives** (*TN*) The number of the normal cells is correctly labelled by the classifier.
$\frac{TN}{Actualfalseclass}$
3) **False Positive** (*FP*) A false positive means that an abnormal leukemia cell was misdiagnosed as an abnormal leukemia cell.
$\frac{FP}{Predictedtrueclass}$
4) **False Negative** (*FN*) Normal cells that were mislabeled as abnormal cell.
$\frac{FN}{Predictedfalseclass}$

Based on evaluation metrics parameters, the confusion matrix is computed to evaluate the classification error of the proposed lightweight EfficientNet-B3. In Fig. 7, it is clearly shown that our proposed lightweight EfficientNet-B3 performed well on the unseen data for both classes, such as leukemia and normal classes. All class (leukemia) is identified as positive, and normal samples are labelled as negative. The proposed classifier correctly predicted 523 out of those 534 sample images. Furthermore, our proposed classifier accurately classified 358 samples as *TP* (leukemia) out

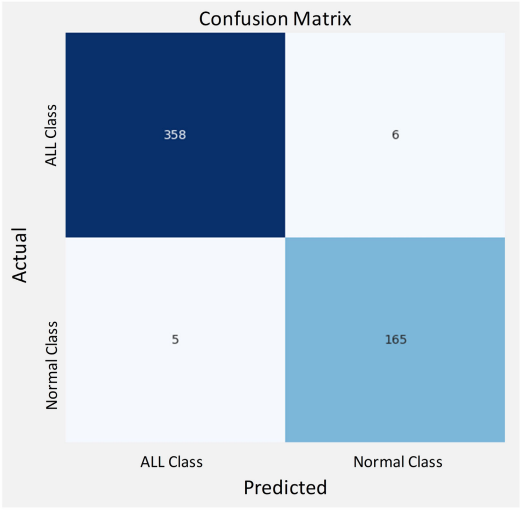

FIGURE 7. Confusion metrics of the proposed lightweight EfficientNet-B3.

of 364. In this way, it is found that our proposed classifier classifies 6 samples as *FN*, which actually belong to the *TN* class. Furthermore, it is found that our proposed classifier predicted 165 samples as a normal class (such as *TN*) out of 171. 5 samples out of 171 are labelled as *FP*, which actually belongs to the negative class but is incorrectly classified as positive. Overall, our proposed classifier performed well in terms of accurate classification to produce a small error, which indicates that our proposed classifier is reliable and efficient in performing binary classification in terms of leukemia and normal.

Furthermore, different performance metrics can be computed based on the evaluation (confusion) matrix to evaluate the effectiveness of the proposed classifier and compare the classification performance of the proposed classifier with existing state-of-the-art classifiers. Table 4 summarizes the evaluation metrics to evaluate and compare the effectiveness of the proposed classifier with existing state-of-the-art classifiers. The correct detection is the difference between *TP* and *TN*. Positive prediction means the actual label and predicted label are both positive and negative prediction means both are negative. For example, if we submit an image for testing and its original label is leukemia, and the prediction is a normal result, it will be considered as *FP*. *FP* label predicts a negative outcome, while a *FN* label predicts the opposite. False positives and false negatives are the values at which the model accuracy decreases. According to our trained model, most samples correctly identified their class, while very few samples had false positives and predicted false negatives.

In addition, Table 6 shows a comparative analysis of the proposed and the state-of-the-art classifiers to evaluate and compare the performance in terms of accuracy, precision, recall, and f1 score. The comparison analysis indicates the proposed classifier achieved an accuracy of 99.31%, which is significantly better than the state-of-the-art classifiers, such as VGG19, Xception, ResNet50, and Efficient NetB0.

TABLE 4. Evaluation metrics equations with a detailed description.

Observe	Equations	Details Description
$Accuracy$	$\frac{TP+TN}{TP+TN+FP+FN}$	The ability of the classifier to correctly classify the class label.
$Precision$	$\frac{TP}{TP+FP}$	This measure indicates how many positive classes are correct.
$Recall$	$\frac{TP}{TP+FN}$	The metric indicates how many were correctly classified out of all positive class.
$F1-socre$	$2 * \frac{\text{Precision} * \text{Recall}}{\text{Precision} + \text{Recall}}$	This metrics use a percentage of the balance between precision and recall

TABLE 5. Evaluation percentage (%) analysis of the proposed and baseline DL classifiers using binary-class leukemia dataset.

Model	Accuracy	Precision	Recall	F1 Score
VGG19	91.33	83.10	91.00	91.84
Xception	93.90	89.00	92.10	95.00
ResNet50	95.10	91.63	94.10	96.90
Efficient NetB0	97.50	91.63	97.00	92.89
Proposed	**99.31**	**95.62**	**98.00**	**99.35**

Similarly, the detection rate of the proposed classifier is 95.62%, which indicates that the proposed classifier efficiently detects patients having leukemia cancer. In addition, the recall of the proposed classifier is 98%, slightly better than the Efficient NetB0 classifier. In addition, our proposed classifier accurately performed and achieved the F1 score of 99.35%, which is high among the implemented classifiers. Hence, our proposed classifier is efficiently performed well to enhance the classification performance for subjects with leukemia or normal cancer.

Additionally, according to the given predicted falsies, the conditional probability for predicted positive being predicted as positive values is 0.986 calculated using the formula given in equation 5. Similarly, the conditional probability for the negative values being predicted as negative is 0.970 following equation 6. The high values of the conditional probability suggest higher performance confidence in the predicted models further added by the accuracy, recall, F1-score, and precision.

$$P(A \mid B) = \frac{P(A \cap B)}{P(B)} \tag{5}$$

$$P(B \mid A) = \frac{P(B \cap A)}{P(A)} \tag{6}$$

TABLE 6. Evaluation percentage (%) analysis of the proposed and baseline DL classifiers using multi-class leukemia dataset.

Model	Accuracy	Precision	Recall	F1 Score
VGG19	89.84	91.21	93.19	92.19
Xception	92.03	94.24	93.67	93.96
ResNet50	93.63	95.76	94.61	95.18
Efficient NetB0	93.90	95.73	95.15	95.44
Proposed	**96.81**	**97.27**	**97.87**	**97.57**

Moreover, our proposed model is evaluated on a multi-class leukaemia dataset to ensure the generalization and effectiveness of the proposed research study. The evaluation results indicate that the proposed classifier achieved better classification performance compared to the state-of-the-art classifiers. In addition, our proposed classifier achieved a detection rate of 97.27%, which is high compared to the other implemented classifiers for multi-class classification of leukemia using the ALL images dataset. Furthermore, our proposed classifier achieved a better F1 score of 97.57% compared to the existing DL classifiers for leukemia classification. Hence, our proposed classifier is reliable and generalized to make an accurate multi-class classification of leukemia.

C. DISCUSSION

This section aims to analyze the effectiveness of the proposed lightweight classifier for leukemia detection. In this study, different baseline DL classifiers are implemented to analyze the significance of the proposed research study. In addition, different evaluation matrices are utilized to evaluate and compare the performance of the proposed and baseline state-of-the-art classifiers. Fig. 8 visualizes the evaluation of the proposed and state-of-the-art classifiers to highlight the significance of the proposed research study. The effectiveness analysis indicates that the proposed classifier improved the classification accuracy by 7.98%, 5.41%, 4.21%, and 1.81% compared to the VGG19, Xception, ResNet50 and EfficientNet-B0, respectively. Similarly, our proposed classifier significantly improved the detection rate by 12.52% compared to the baseline VGG19 classifier. In addition, it is also found that the proposed model improved the detection rate compared to the Xception, ResNet50 and EfficientNet-B0 by 6.62%, 3.99%, and 3.99%, respectively. Furthermore, in terms of recall, our proposed classifier outperformed and significantly improved the performance by 7% and 5.90% compared to the VGG19 and Xception classifiers. Similarly, our proposed classifier improved recall by 3.9% and 1% compared to the ResNet50 and EfficientNet-B0 classifiers. In addition, our proposed classifier significantly improved the F1 score by 7.51% and 6.46% compared to the VGG19 and EfficientNet-B0 classifiers to highlight the effectiveness of the proposed research study. It is also found that the proposed classifier improved the F1 score by 4.35% and 2.45%

FIGURE 8. Effectiveness analysis of the proposed and baseline classifiers for leukemia detection using binary classification dataset.

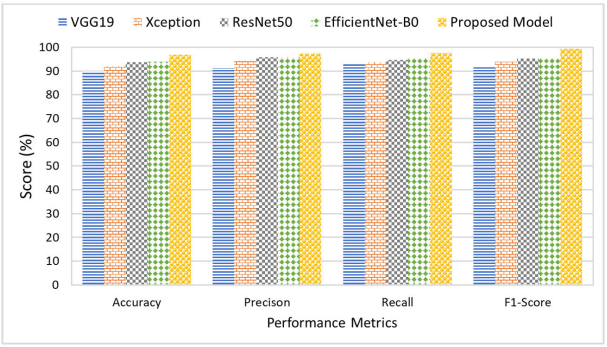

FIGURE 9. Effectiveness analysis of the proposed and baseline classifiers for leukemia detection using multi-class classification dataset.

compared to the Xception and ResNet50 classifiers. Hence, our proposed classifier is robust and reliable to significantly enhance the performance of leukemia detection compared to the state-of-the-art classifiers.

Furthermore, Fig. 9 presents an effectiveness analysis of the proposed and baseline DL classifiers for the multi-class classification of leukemia. The effectiveness analysis shows that the proposed classifier achieved an accuracy of 6.97% better than the VGG19 classifier. Similarly, our proposed classifier improved the accuracy of 4.78%, 3.18%, and 2.91% compared to the Xception, ResNet50, and EfficientNet-B0 classifiers. In addition, our proposed classifier improved the detection rate compared to the baseline DL models. Furthermore, our proposed classifier improved F1 score by 5.38%, 3.61%, 2.39%, and 2.13% compared to the VGG19, Xception, ResNet50, and EfficientNet-B0 (ENB0) classifiers. The effectiveness analysis finding indicates that the proposed classifier performed slightly better for binary classification compared to the multi-class classification datasets. However, our proposed classifier performed better than the existing classifiers for the multi-class classification of leukemia.

In addition, Fig. 10 shows a comparative analysis of the detection rate for binary and multi-class leukemia detection using proposed and existing DL classifiers. The comparative analysis indicates that the detection rate of the proposed classifier is better compared to the existing classifiers. The

FIGURE 10. Comparative analysis of detection rate for leukemia detection using binary and multi-class classification dataset.

TABLE 7. Efficiency analysis of proposed and baseline classifiers using *C_NMC_*2019 dataset.

#	Classifier	Trainable Parameters
1	VGG19	45,716,545
2	Xception	22,518,453
3	ResNet50	31,925,240
4	Efficient-NetB0	167,984,681
5	**Proposed**	11,093,290

analysis also indicates that the detection rate of the proposed classifier is slightly better for the multi-class classification of leukemia compared to the binary classification of leukemia. Furthermore, it is also found that the detection rate of all implemented classifiers is improved for the multi-class classification of leukemia compared to the binary classification.

Furthermore, Table 7 shows a detailed comparison of the trainable parameters of the proposed and baseline classifiers to evaluate the efficiency of the proposed research study. The trainable parameters include weights and biases to evaluate the efficiency of the proposed and baseline classifiers. The analysis indicates that the proposed lightweight classifier is required a small number of trainable parameters compared to other implemented classifiers. Therefore, it is proved that our proposed classifier is efficient because it drastically reduces the computational cost in terms of trainable parameters to enhance the efficiency of the proposed research study for leukemia detection.

The algorithm suggested in this article is compared to other blood cell Deep-learning classification algorithms with the same dataset used in this study to classify leukemia blood cell images. Gao et al. [62] proposed an EfficientNet-B0 architecture. Additionally, it is evaluated compared to various CNN models, including ResNet and Inception V3. The experiment results indicate that the authors' presented method has the highest classification accuracy at 95.18%. Using a CNN-based ECA module, Ullah et al. [63] improved the CNN hyper-parameters and achieved 91.10% accuracy on the dataset. To detect images of cells, in [64], the authors proposed a vision transfer model and achieved an accuracy of

TABLE 8. Accuracy comparison with previous work.

Ref	Year	Method	Accuracy
[62]	2021	EfficientNetB0	95.18%
[63]	2021	CNN based ECA module	91.10%
[64]	2022	Vision Transformer	88.20 %
[65]	2022	Majority Voting Technique	98.50%
[66]	2023	CNN Model based Tversky Loss Function	99.01%
Proposed	**2023**	**EfficientNet-B3**	**99.31%**

88.20% on the dataset. On the entire data set [65], accuracy was 98.50% majority. The voting Technique is also used to compare the model's performance in terms of computation time and accuracy. According to the experimental findings, trained the model more quickly, and Ansari et al. [66] used CNN model-based Tversky loss function to display the detailed comparison results.

V. CONCLUSION

Our research paper presented image classification techniques based on deep learning for classifying white blood cells image data. We used a pre-trained model to accurately classify ALL and normal cells to predict ALL. In addition, this research study used two datasets to evaluate the performance and generalization of the DL-assisted pre-trained robust classifiers. First, the C_NMC_19 dataset was considered as a binary class dataset to classify both ALL cancer cells and normal cells. Second, the ALL dataset was used as a multi-class dataset to evaluate and compare the performance of the DL-assisted pre-trained classifiers. Furthermore, different evaluation measures were used to analyze the effectiveness of the pre-trained classifiers and also compared the performance and efficiency to find the best classifier for leukemia detection. Based on comparative analysis, it is found that the EfficientNet-B3 significantly performed well on both binary and multi-class classification of leukemia and achieved a detection rate of 95.62% and 97.27% for binary and multi-classification datasets. Furthermore, EfficientNet-B3, as a robust DL classifier, performed well as an individual state-of-the-art and achieved an accuracy of 99.31%, precision of 95.62%, recall of 98.00%, and F1 score of 99.35% using C-NMC-19 dataset (binary classes). In addition, a multi-class ALL dataset was employed to evaluate the generalization of DL classifiers and it found that EfficientNet-B3 outperformed the counterpart DL classifiers. Based on multi-class dataset analysis, EfficientNet-B3 achieved an accuracy of 96.81%, precision of 97.27%, recall of 97.87%, and F1 score of 97.57%. In addition, based on a detailed comparison of the detection rate of the EfficientNet-B3 and ensemble classifiers, it was found that the EfficientNet-B3 achieved a better detection rate than ensemble classifiers for both

binary and multi-class classification of leukemia. Moreover, EfficientNet-B3 not only achieved better performance but also had high efficiency by utilizing less amount of trainable parameters to reduce the computational complexity compared to other implemented pre-trained DL classifiers.

Future work will be conducted to utilize explainable AI (for example, SHAP) to enhance the transparency and adaptability of the proposed lightweight EfficientNet-B3 and other pre-trained DL classifiers for leukaemia detection. Furthermore, the performance of the DL classifiers can be enhanced by determining the optimal set of hyper-parameters, such as the number of hidden layers, batch size, activation function, etc. There is still a need for a practical solution to improve image classification performance. Thus, future researchers can explore a variety of new deep-learning models.

REFERENCES

[1] D. T. O. Yeung, M. P. Osborn, and D. L. White, "B-cell acute lymphoblastic leukaemia: Recent discoveries in molecular pathology, their prognostic significance, and a review of the current classification," *Brit. J. Haematology*, vol. 197, no. 1, pp. 13–27, Apr. 2022.

[2] American Cancer Society. (2022). *Leukemia Blood Cancer*. [Online]. Available: https://www.cancer.org/cancer/acute-lymphocytic-leukemia/about/key-statistics.html

[3] U. Joshi, S. Khanal, U. Bhetuwal, A. Bhattarai, P. Dhakal, and V. R. Bhatt, "Impact of insurance on overall survival in acute lymphoblastic leukemia: A SEER database study," *Clin. Lymphoma Myeloma Leukemia*, vol. 22, no. 7, pp. 477–484, Jul. 2022.

[4] N. V. Frey, "Approval of brexucabtagene autoleucel for adults with relapsed and refractory acute lymphocytic leukemia," *Blood*, vol. 140, no. 1, pp. 11–15, Jul. 2022.

[5] J. L. McNeer and K. Schmiegelow, "Management of CNS disease in pediatric acute lymphoblastic leukemia," *Current Hematologic Malignancy Rep.*, vol. 17, no. 1, pp. 1–14, Feb. 2022.

[6] A. P. Stein, R. E. Norris, and J. R. Shah, "Pediatric acute lymphoblastic leukemia presenting with periorbital edema," *Otolaryngol. Case Rep.*, vol. 9, pp. 11–14, Nov. 2018.

[7] Z. Ahmed and A. Ahmed, "Evaluation of serum level of lymphoid enhancer-binding factor-1 and its relation with clinico-hematological and prognostic parameters in pediatric patients with acute lymphoblastic leukemia," *Iraqi J. Hematology*, vol. 11, no. 1, p. 45, 2022.

[8] H. Mohamed, R. Omar, N. Saeed, A. Essam, N. Ayman, T. Mohiy, and A. AbdelRaouf, "Automated detection of white blood cells cancer diseases," in *Proc. 1st Int. Workshop Deep Represent. Learn. (IWDRL)*, Mar. 2018, pp. 48–54.

[9] S. A. Yazdan, R. Ahmad, N. Iqbal, A. Rizwan, A. N. Khan, and D.-H. Kim, "An efficient multi-scale convolutional neural network based multi-class brain MRI classification for SaMD," *Tomography*, vol. 8, no. 4, pp. 1905–1927, Jul. 2022.

[10] T. Shahzad, K. Iqbal, M. A. Khan, and N. Iqbal, "Role of zoning in facial expression using deep learning," *IEEE Access*, vol. 11, pp. 16493–16508, 2023.

[11] J. Amin, M. Sharif, M. A. Anjum, A. Siddiqa, S. Kadry, Y. Nam, and M. Raza, "3D semantic deep learning networks for leukemia detection," Tech Sci. Press, Henderson, NV, USA, Tech. Rep., 2021.

[12] J. Amin, M. A. Anjum, M. Sharif, S. Kadry, Y. Nam, and S. Wang, "Convolutional bi-LSTM based human gait recognition using video sequences," *Comput., Mater. Continua*, vol. 68, no. 2, pp. 2693–2709, 2021.

[13] S. Saleem, J. Amin, M. Sharif, M. A. Anjum, M. Iqbal, and S.-H. Wang, "A deep network designed for segmentation and classification of leukemia using fusion of the transfer learning models," *Complex Intell. Syst.*, vol. 8, no. 4, pp. 3105–3120, Aug. 2022.

[14] Q. Zhang, L. Sun, J. Chen, M. Zhou, M. Hu, Y. Wen, and Q. Li, "Speeded-up robust features-based image mosaic method for large-scale microscopic hyperspectral pathological imaging," *Meas. Sci. Technol.*, vol. 32, no. 3, Mar. 2021, Art. no. 035503.

[15] A. M. Noor, Z. Zakaria, A. M. Noor, and A. N. Norali, "Classification of white blood cells based on surf feature," *Suranaree J. Sci. Technol.*, vol. 28, no. 1, 2021.

[16] L. C. de Faria, L. F. Rodrigues, and J. F. Mari, "Cell classification using handcrafted features and bag of visual words," in *Proc. Anais do XIV Workshop de Visão Computacional*, 2018.

[17] S. Gheisari, D. Catchpoole, A. Charlton, Z. Melegh, E. Gradhand, and P. Kennedy, "Computer aided classification of neuroblastoma histological images using scale invariant feature transform with feature encoding," *Diagnostics*, vol. 8, no. 3, p. 56, Aug. 2018.

[18] A. Abhishek, R. K. Jha, R. Sinha, and K. Jha, "Automated classification of acute leukemia on a heterogeneous dataset using machine learning and deep learning techniques," *Biomed. Signal Process. Control*, vol. 72, Feb. 2022, Art. no. 103341.

[19] S. Mishra, B. Majhi, P. K. Sa, and L. Sharma, "Gray level co-occurrence matrix and random forest based acute lymphoblastic leukemia detection," *Biomed. Signal Process. Control*, vol. 33, pp. 272–280, Mar. 2017.

[20] E. K. Ruby, "Automatic detecftion of white blood cancer from blood cells using novel machine lerning techniques," in *Proc. 8th Int. Conf. Adv. Comput. Commun. Syst. (ICACCS)*, Mar. 2022, pp. 79–85.

[21] Z. Khan, W. Mumtaz, A. S. Mumtaz, S. Bhattacharjee, and H.-C. Kim, "Multiclass-classification of algae using DC-GAN and transfer learning," in *Proc. 2nd Int. Conf. Image Process. Robot. (ICIPRob)*, Mar. 2022, pp. 1–6.

[22] R. Bram and M. Nasstrom, "Detecting nucleated cells in bone marrow smears using deep learning," M.S. thesis, Centre Math. Sci. Math., Lunda Univ., Lunda, Sweden, 2021.

[23] F. Nesti, G. Rossolini, S. Nair, A. Biondi, and G. Buttazzo, "Evaluating the robustness of semantic segmentation for autonomous driving against real-world adversarial patch attacks," in *Proc. IEEE/CVF Winter Conf. Appl. Comput. Vis. (WACV)*, Jan. 2022, pp. 2280–2289.

[24] S. M. Badawy, A. E.-N.-A. Mohamed, A. A. Hefnawy, H. E. Zidan, M. T. GadAllah, and G. M. El-Banby, "Automatic semantic segmentation of breast tumors in ultrasound images based on combining fuzzy logic and deep learning—A feasibility study," *PLoS ONE*, vol. 16, no. 5, May 2021, Art. no. e0251899.

[25] M. H. Bendiabdallah and N. Settouti, "A comparison of U-Net backbone architectures for the automatic white blood cells segmentation," *WAS Sci. Nature (WASSN)*, vol. 4, no. 1, 2021.

[26] S. P. Sunny, A. I. Khan, M. Rangarajan, A. Hariharan, P. Birur, N. Shah, M. A. Kuriakose, and A. Suresh, "Oral epithelial cell segmentation from fluorescent multichannel cytology images using deep learning," *Comput. Methods Programs Biomed.*, vol. 227, Dec. 2022, Art. no. 107205.

[27] S. Alagu and K. B. Bagan, "Computer assisted classification framework for detection of acute myeloid leukemia in peripheral blood smear images," in *Innovations in Computational Intelligence and Computer Vision*. Cham, Switzerland: Springer, 2021, pp. 403–410.

[28] H. Abedy, F. Ahmed, M. N. Q. Bhuiyan, M. Islam, N. Y. Ali, and M. Shamsujjoha, "Leukemia prediction from microscopic images of human blood cell using HOG feature descriptor and logistic regression," in *Proc. 16th Int. Conf. ICT Knowl. Eng.*, Nov. 2018, pp. 1–6.

[29] A. Molina, S. Alférez, L. Boldu, A. Acevedo, J. Rodellar, and A. Merino, "Sequential classification system for recognition of malaria infection using peripheral blood cell images," *J. Clin. Pathol.*, vol. 73, no. 10, pp. 665–670, Oct. 2020.

[30] J. M. Patel and N. C. Gamit, "A review on feature extraction techniques in content based image retrieval," in *Proc. Int. Conf. Wireless Commun., Signal Process. Netw. (WiSPNET)*, Mar. 2016, pp. 2259–2263.

[31] V. Wasson, "An efficient content based image retrieval based on speeded up robust features (SURF) with optimization technique," in *Proc. 2nd IEEE Int. Conf. Recent Trends Electron., Inf. Commun. Technol. (RTEICT)*, May 2017, pp. 730–735.

[32] Y. Li, Q. Li, Y. Liu, and W. Xie, "A spatial–spectral SIFT for hyperspectral image matching and classification," *Pattern Recognit. Lett.*, vol. 127, pp. 18–26, Nov. 2019.

[33] S. Li, Z. Wang, and Q. Zhu, "A research of ORB feature matching algorithm based on fusion descriptor," in *Proc. IEEE 5th Inf. Technol. Mechatronics Eng. Conf. (ITOEC)*, Jun. 2020, pp. 417–420.

[34] S. Saleem, J. Amin, M. Sharif, G. A. Mallah, S. Kadry, and A. H. Gandomi, "Leukemia segmentation and classification: A comprehensive survey," *Comput. Biol. Med.*, vol. 150, Nov. 2022, Art. no. 106028.

[35] J. Amin, M. Sharif, M. Raza, T. Saba, and A. Rehman, "Brain tumor classification: Feature fusion," in *Proc. Int. Conf. Comput. Inf. Sci. (ICCIS)*, 2019, pp. 1–6.

[36] J. Ma, X. Jiang, A. Fan, J. Jiang, and J. Yan, "Image matching from handcrafted to deep features: A survey," *Int. J. Comput. Vis.*, vol. 129, pp. 23–79, Aug. 2020.
[37] S. M. Naqi, M. Sharif, M. Yasmin, and S. L. Fernandes, "Lung nodule detection using polygon approximation and hybrid features from CT images," *Current Med. Imag. Rev.*, vol. 14, no. 1, pp. 108–117, Dec. 2017.
[38] F. Shi, J. Wang, J. Shi, Z. Wu, Q. Wang, Z. Tang, K. He, Y. Shi, and D. Shen, "Review of artificial intelligence techniques in imaging data acquisition, segmentation, and diagnosis for COVID-19," *IEEE Rev. Biomed. Eng.*, vol. 14, pp. 4–15, 2020.
[39] M. L. Claro, R. D. M. S. Veras, A. M. Santana, L. H. S. Vogado, G. B. Junior, F. N. S. D. Medeiros, and J. M. R. S. Tavares, "Assessing the impact of data augmentation and a combination of CNNs on leukemia classification," *Inf. Sci.*, vol. 609, pp. 1010–1029, Sep. 2022.
[40] C. Kanumuri and C. R. Madhavi, "A survey: Brain tumor detection using MRI image with deep learning techniques," in *Smart and Sustainable Approaches for Optimizing Performance of Wireless Networks: Real-time Applications*. Hoboken, NJ, USA: Wiley, 2022, pp. 125–138.
[41] S. Malik, J. Amin, M. Sharif, M. Yasmin, S. Kadry, and S. Anjum, "Fractured elbow classification using hand-crafted and deep feature fusion and selection based on whale optimization approach," *Mathematics*, vol. 10, no. 18, p. 3291, Sep. 2022.
[42] J. Amin, M. Sharif, M. Yasmin, and S. L. Fernandes, "A distinctive approach in brain tumor detection and classification using MRI," *Pattern Recognit. Lett.*, vol. 139, pp. 118–127, Nov. 2020.
[43] J. Amin, M. Sharif, M. Yasmin, and S. L. Fernandes, "Big data analysis for brain tumor detection: Deep convolutional neural networks," *Future Gener. Comput. Syst.*, vol. 87, pp. 290–297, Oct. 2018.
[44] T. Saba, A. S. Mohamed, M. El-Affendi, J. Amin, and M. Sharif, "Brain tumor detection using fusion of hand crafted and deep learning features," *Cogn. Syst. Res.*, vol. 59, pp. 221–230, Jan. 2020.
[45] M. I. Sharif, J. P. Li, J. Amin, and A. Sharif, "An improved framework for brain tumor analysis using MRI based on YOLOv2 and convolutional neural network," *Complex Intell. Syst.*, vol. 7, no. 4, pp. 2023–2036, Aug. 2021.
[46] R. Anand, T. Shanthi, M. Nithish, and S. Lakshman, "Face recognition and classification using GoogleNET architecture," in *Soft Computing for Problem Solving*. Berlin, Germany: Springer, 2020, pp. 261–269.
[47] J. Amin, M. Sharif, E. Gul, and R. S. Nayak, "3D-semantic segmentation and classification of stomach infections using uncertainty aware deep neural networks," *Complex Intell. Syst.*, vol. 8, no. 4, pp. 3041–3057, Aug. 2022.
[48] M. Shahzad, A. I. Umar, M. A. Khan, S. H. Shirazi, Z. Khan, and W. Yousaf, "Robust method for semantic segmentation of whole-slide blood cell microscopic images," *Comput. Math. Methods Med.*, vol. 2020, pp. 1–13, Jan. 2020.
[49] A. Meenakshi, J. A. Ruth, V. Kanagavalli, and R. Uma, "Automatic classification of white blood cells using deep features based convolutional neural network," *Multimedia Tools Appl.*, vol. 81, no. 21, pp. 30121–30142, 2022.
[50] P. Jagadev and H. G. Virani, "Detection of leukemia and its types using image processing and machine learning," in *Proc. Int. Conf. Trends Electron. Informat. (ICEI)*, May 2017, pp. 522–526.
[51] H. M. Osman and S. P. Yaba, "Automated segmentation of acute lymphocytic leukemia (ALL) subtypes by the combination of color space conversion and K-means cluster," *Zanco J. Pure Appl. Sci.*, vol. 34, no. 3, pp. 11–20, 2022.
[52] B. Leng, C. Wang, M. Leng, M. Ge, and W. Dong, "Deep learning detection network for peripheral blood leukocytes based on improved detection transformer," *Biomed. Signal Process. Control*, vol. 82, Apr. 2023, Art. no. 104518.
[53] H. Raji, M. Tayyab, J. Sui, S. R. Mahmoodi, and M. Javanmard, "Biosensors and machine learning for enhanced detection, stratification, and classification of cells: A review," *Biomed. Microdevices*, vol. 24, no. 3, pp. 1–20, Sep. 2022.
[54] M. E. Billah and F. Javed, "Bayesian convolutional neural network-based models for diagnosis of blood cancer," *Appl. Artif. Intell.*, vol. 36, no. 1, Dec. 2022, Art. no. 2011688.
[55] T. G. Devi, N. Patil, S. Rai, and C. S. Philipose, "Survey of leukemia cancer cell detection using image processing," in *Proc. Int. Conf. Comput. Vis. Image Process.* Cham, Switzerland: Springer, 2022, pp. 468–488.
[56] G. Atteia, A. Alhussan, and N. Samee, "BO-ALLCNN: Bayesian-based optimized CNN for acute lymphoblastic leukemia detection in microscopic blood smear images," *Sensors*, vol. 22, no. 15, p. 5520, Jul. 2022.
[57] A. Saeed, S. Shoukat, K. Shehzad, I. Ahmad, A. A. Eshmawi, A. H. Amin, and E. Tag-Eldin, "A deep learning-based approach for the diagnosis of acute lymphoblastic leukemia," *Electronics*, vol. 11, no. 19, p. 3168, Oct. 2022.
[58] M. Tan and Q. Le, "EfficientNet: Rethinking model scaling for convolutional neural networks," in *Proc. Int. Conf. Mach. Learn.*, 2019, pp. 6105–6114.
[59] M. Abadi, P. Barham, J. Chen, Z. Chen, A. Davis, J. Dean, M. Devin, S. Ghemawat, G. Irving, M. Isard, and M. Kudlur, "TensorFlow: A system for large-scale machine learning," in *Proc. 12th USENIX Symp. Operating Syst. Design Implement. (OSDI)*, 2016, pp. 265–283.
[60] N. Iqbal, R. Ahmad, F. Jamil, and D.-H. Kim, "Hybrid features prediction model of movie quality using multi-machine learning techniques for effective business resource planning," *J. Intell. Fuzzy Syst.*, vol. 40, no. 5, pp. 9361–9382, Apr. 2021.
[61] A. Batool and Y.-C. Byun, "An ensemble architecture based on deep learning model for click fraud detection in pay-per-click advertisement campaign," *IEEE Access*, vol. 10, pp. 113410–113426, 2022.
[62] Z. Gao, J. Chung, M. Abdelrazek, S. Leung, W. K. Hau, Z. Xian, H. Zhang, and S. Li, "Privileged modality distillation for vessel border detection in intracoronary imaging," *IEEE Trans. Med. Imag.*, vol. 39, no. 5, pp. 1524–1534, May 2020.
[63] M. Z. Ullah, Y. Zheng, J. Song, S. Aslam, C. Xu, G. D. Kiazolu, and L. Wang, "An attention-based convolutional neural network for acute lymphoblastic leukemia classification," *Appl. Sci.*, vol. 11, no. 22, p. 10662, Nov. 2021.
[64] P. Cho, S. Dash, A. Tsaris, and H.-J. Yoon, "Image transformers for classifying acute lymphoblastic leukemia," in *Proc. SPIE*, vol. 12033, pp. 633–639, Apr. 2022.
[65] M. Ghaderzadeh, A. Hosseini, F. Asadi, H. Abolghasemi, D. Bashash, and A. Roshanpoor, "Automated detection model in classification of B-lymphoblast cells from normal B-lymphoid precursors in blood smear microscopic images based on the majority voting technique," *Sci. Program.*, vol. 2022, pp. 1–8, Jan. 2022.
[66] S. Ansari, A. H. Navin, A. B. Sangar, J. V. Gharamaleki, and S. Danishvar, "A customized efficient deep learning model for the diagnosis of acute leukemia cells based on lymphocyte and monocyte images," *Electronics*, vol. 12, no. 2, p. 322, Jan. 2023.

AMREEN BATOOL received the bachelor's degree from GC University, Pakistan, the M.C.S. degree from the Virtual University of Pakistan, and the M.S. degree in computer science and technology from Tiangong University, Tianjin, China, in 2021. She is currently pursuing the Ph.D. degree with the Department of Electronic Engineering, Jeju National University, South Korea. She is a Project Coordinator with EUT Global Ltd. Her main role is to coordinate with clients and field engineers to plan project delivery. Her research interests include machine learning, deep learning, and blockchain technology.

YUNG-CHEOL BYUN received the B.S. degree from Jeju National University, in 1993, and the M.S. and Ph.D. degrees from Yonsei University, in 1995 and 2001, respectively. He was a Special Lecturer with Samsung Electronics, from 2000 to 2001. From 2001 to 2003, he was a Senior Researcher with the Electronics and Telecommunications Research Institute (ETRI). He was promoted to join Jeju National University as an Assistant Professor, in 2003, where he is currently an Associate Professor with the Computer Engineering Department. His research interests include AI machine learning, pattern recognition, blockchain, deep learning-based applications, big data, knowledge discovery, time series data analysis and prediction, image processing, medical applications, and recommendation systems.